Phototransistors Based on InP HEMTs and Their Applications to Millimeter-Wave Radio-on-Fiber Systems

Chang-Soon Choi, *Student Member, IEEE*, Hyo-Soon Kang, Woo-Young Choi, *Member, IEEE*, Dae-Hyun Kim, and Kwang-Seok Seo

***Abstract*—Phototransistors based on InP high electron-mobility transistors (HEMTs) are investigated for millimeter-wave radio-on-fiber system applications. By clarifying the photodetection mechanism in InP HEMTs, the phototransistor internal gain is determined. We present their use as millimeter-wave harmonic optoelectronic mixers and characterize them at the 60-GHz band. In order to evaluate the InP HEMT optoelectronic mixer performance, internal conversion gain is introduced and a maximum of 17 dB is obtained for 60-GHz harmonic optoelectronic up-conversion. Utilizing them, we construct a 60–GHz radio-on-fiber system and demonstrate 622-Mb/s data transmission over 30-km single-mode fiber and 3-m free space at 60-GHz band.**

***Index Terms*—High electron-mobility transistor (HEMT), optically controlled microwave device, optoelectronic mixer, photodetector, phototransistor.**

I. Introduction

MILLIMETER-WAVE frequency bands around 60 GHz have been of much interest in broad-band wireless-access network applications because of their wide transmission bandwidth and spectral characteristics including high atmospheric loss and unlicensed band. However, their use is not yet widespread due to the difficulties in millimeter-wave generation, transmission, and processing. With the development of fiber-optic technologies, radio-on-fiber systems that utilize optical fibers as low-loss and highly flexible transmission medium have been investigated as a solution for these problems [1], [2]. In a millimeter-wave radio-on-fiber system, a large number of base stations are located within the coverage of a single central office in order to compensate high transmission loss. Therefore, it is important to come up with low-cost base-station architecture for practical implementation of these radio-on-fiber systems.

There are several approaches to simplify base-station architecture in millimeter-wave radio-on-fiber system. One attractive solution is to move the millimeter-wave components away from numerous base stations to a single central office [2], [3]. Since millimeter-wave signals are optically generated at a central office and transmitted over fiber, base-station architecture can be made up of only a photodetector, power amplifier, and radiation antenna. However, the optical generation of a millimeter wave still remains as a challenging task. In addition, chromatic fiber dispersion, which induces carrier-to-noise penalty and phase-noise degradation, is a limiting factor for increasing transmission distance in this configuration [4]. Another approach is one-chip integration of photonic and millimeter-wave components including a frequency mixer and local oscillator (LO) [5], [6]. In this scheme, called the remote up-conversion system, IF modulated optical signals are transmitted, and remotely up-converted to millimeter wave at base station [7]. Although it mitigates the above-mentioned problems and provides compatibility to wavelength division multiplexing (WDM) networks, complex base-station architecture is inevitable, thus, the monolithic integration on a single substrate has been regarded as an ultimate goal for simple and cost-effective base-station architecture in these remote up-conversion systems.

Three-terminal phototransistors based on metal–semiconductor field-effect transistors (MESFETs), high electron-mobility transistors (HEMTs), and heterojunction bipolar transistors (HBTs) are useful devices for these optoelectronic integrations [5]–[10]. It is because they can be utilized as not only phototransistors providing high internal gain, but also optoelectronic mixers, which simultaneously perform photodetection and frequency up-conversion in a single device. In addition, these phototransistors are fully compatible to monolithic-microwave integrated-circuit (MMIC) processes.

Among various kinds of phototransistors, indium-phosphide (InP) HEMTs have numerous advantages for these MMIC-compatible optoelectronic integration. Since large conduction band discontinuity at the InAlAs/InGaAs heterojunction interface produces high two-dimensional electron gas densities in the InGaAs channel, an InP HEMT exhibits extremely high electron mobility without suffering impurity scattering, resulting in high-frequency performance up to the millimeter-wave regime [11]. In addition, the InGaAs channel with high indium contents ($\geq$53%) performs the photodetection to 1.55-μm lightwave and then the detected signals are amplified by field-effect transistor (FET) operation [12], [13]. Since the InP substrate and InAlAs buffer layer are transparent to 1.55-μm lightwave, additional efforts for an optical window in the HEMT are not required if backside illumination through the InP substrate is applied.

Manuscript received April 21, 2004; revised August 25, 2004. This work was supported by the Ministry of Science and Technology of Korea under the National Research Laboratory Program.

C.-S. Choi, H.-S. Kang, and W.-Y. Choi are with the Department of Electrical and Electronic Engineering, Yonsei University, Seoul 120-749, Korea (e-mail: wchoi@yonsei.ac.kr).

D.-H. Kim and K.-S. Seo are with the School of Electrical Engineering, Seoul National University, Seoul 151-742, Korea.

Digital Object Identifier 10.1109/TMTT.2004.839323

0018-9480/$20.00 © 2005 IEEE

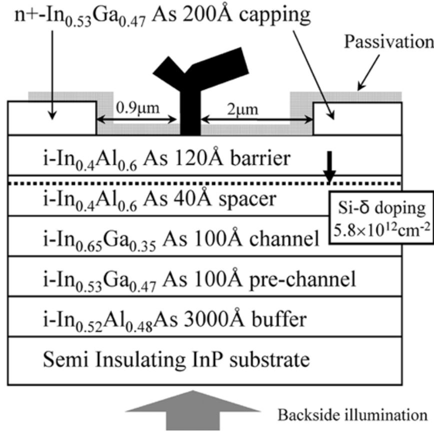

Fig. 1. Schematic cross section of the fabricated InP HEMT having the $In_{0.65}Ga_{0.35}$ As pseudomorphic channel.

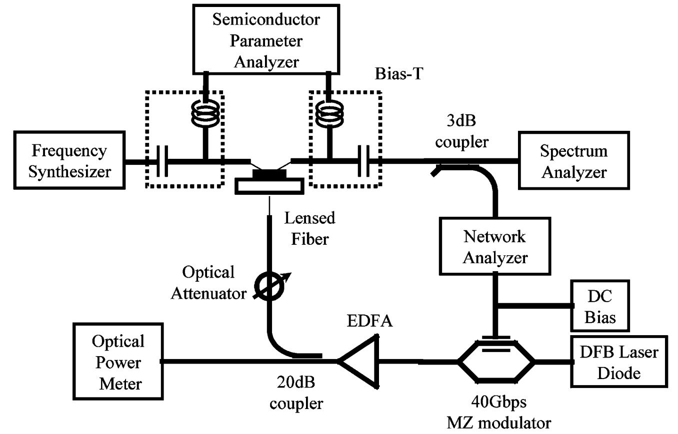

Fig. 2. Experimental setup for the characterization of the InP HEMT as a phototransistor. Backside illumination is applied through an InP substrate to improve optical coupling efficiency.

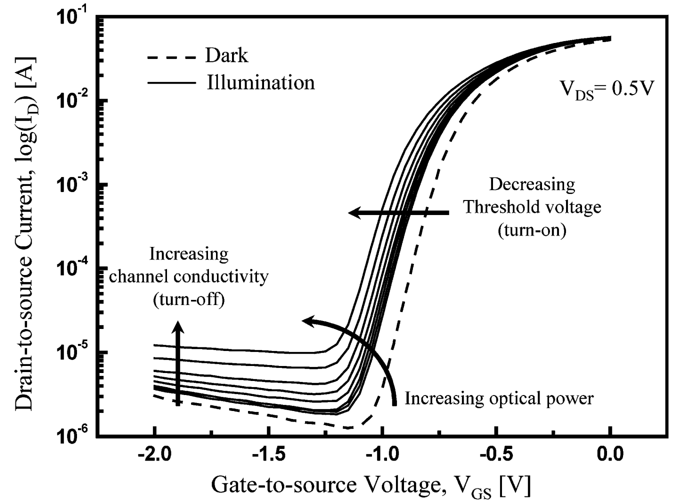

Fig. 3. Drain currents (I_D) as a function of gate-to-source voltages $(V_{\rm GS})$ for the InP HEMT under dark and illuminated conditions at the drain-to-source voltage $(V_{\rm DS})$ of 0.5 V. The incident optical powers increases from -6 to 15 dBm with the step of 3 dB.

In this paper, we investigate phototransistors based on InP HEMTs and demonstrate their applicability for 60-GHz radio-on-fiber systems. In Section II, two types of photodetection mechanisms are identified and the phototransistor internal gain of the InP HEMT is determined. Section III describes their use as harmonic optoelectronic mixers, which combine the functions of photodetection, frequency up-conversion, and LO frequency multiplication in a single HEMT. Such optoelectronic mixer performance characteristics as internal conversion gain and usable LO ranges are also investigated. In Section IV, we present the experimental demonstration of 622-Mb/s data transmission in a 60-GHz remote up-conversion radio-on-fiber system utilizing an InP HEMT harmonic optoelectronic mixer and evaluate its link performance.

II. Photodetection Mechanism of InP HEMT

The schematic cross section of a fabricated InP HEMT is illustrated in Fig. 1. The epitaxial layers were grown on semi-insulating InP substrate by using molecular beam epitaxy (MBE). They are made up of, from bottom to top, 300-nm $In_{0.52}Al_{0.48}As$ buffer layer, 10-nm $In_{0.53}Ga_{0.47}As$ sub-channel, 10-nm $In_{0.65}Ga_{0.35}As$ pseudomorphic channel layers, 4-nm $In_{0.4}Al_{0.6}As$ spacer layer with Si-delta doping (5.8×10^{12} cm^{-2}), 12-nm $In_{0.4}Al_{0.6}As$ barrier layer, and 20-nm n+ $In_{0.53}Ga_{0.47}As$ capping layers. Strained barrier ($In_{0.4}Al_{0.6}As$) and strained channel ($In_{0.65}Ga_{0.35}As$) were adopted to reduce gate leakage current and improve carrier transport properties. The InP HEMT device used for our investigation has a gate length of 0.1 μm, source-to-gate spacing of 0.9 μm, and drain-to-gate spacing of 2 μm. From the dc measurements, the maximum transconductance of 720 mS/mm is obtained. Scattering-parameter measurements show that current–gain cutoff frequency (f_T) and maximum frequency of oscillation $(f_{\max})$ are 148 and 165 GHz, respectively, at the gate-to-source voltage $(V_{\rm GS})$ of -0.5 V and the drain-to-source voltage $(V_{\rm DS})$ of 1.0 V.

Fig. 2 shows the experimental arrangements for the characterization of InP HEMT-based phototransistor. The distributed feedback (DFB) laser diode whose wavelength is 1552 nm is used as an optical source. After optical amplification by an erbium-doped fiber amplifier (EDFA), the lightwave is illuminated from the backside of the InP substrate using a single-mode lensed fiber, which provides coupling efficiency less than 10%. Since the InP substrate and $In_{0.52}Al_{0.48}As$ buffer layer are transparent to 1.55-μm lightwave, optical absorption occurs only at $In_{0.65}Ga_{0.35}$ As and $In_{0.53}Ga_{0.47}$ As channel layers. All measurements are performed in the common-source configuration by utilizing on-wafer ground–signal–ground (GSG) probes.

We first investigate the photodetection mechanism in InP HEMT and characterize its internal gain provided by phototransistor operation. Fig. 3 shows the drain currents (I_D) as a function of $V_{\rm GS}$ under dark and illuminated conditions at the $V_{\rm DS}$ of 0.5 V. The solid line indicates $I_{\rm D}$ under illumination and the dashed line in the dark. Incident optical power to InP HEMT increases from -6 to 15 dBm with the step of 3 dB, which were measured at the end of lensed fiber. When $V_{\rm GS}$ is higher than the threshold voltage, the InP HEMT exhibits negative shifts in threshold voltage, as well as increases in I_D with increasing incident optical power. This is well known to

be due to photovoltaic effects, which are attributed to photogenerated holes diminishing the potential barrier between source and channel [12], [13]. Since the photovoltaic effects effectively modulate the gate voltage, they provide intrinsic gain by FET operation and make the InP HEMT operates as a phototransistor. However, even when $V_{\rm GS}$ is lower than the threshold voltage (turn-off state), it can be observed that I_D slightly increases as increasing optical power. This is due to the photoconductive effects in which photogenerated electrons increase the channel conductivity, which results in increased I_D. As we reported in [14], these photodetection mechanisms can be affirmed by measuring the dependence of photocurrents on input optical powers at each condition. The photocurrent caused by the photovoltaic effect is a logarithmic function of input optical power expressed as

$$\begin{aligned} I_{\rm PV} &= G_m \cdot \Delta V_{\rm TH} \\ &= G_m \cdot \frac{nkT}{q} \ln\left(1 + \frac{q\eta P_{\rm opt}}{I_{\rm dark} \cdot h\nu}\right) \\ &= A \cdot \ln\left(1 + B \cdot P_{\rm opt}\right) \end{aligned} \tag{1}$$

where $I_{\rm PV}$ is the photocurrent by the photovoltaic effect, G_m is the intrinsic transconductance, $\Delta V_{\rm TH}$ is the threshold voltage shift, kT/q is the thermal voltage, n is the ideality factor, η is the quantum efficiency, $I_{\rm dark}$ is the dark current for hole, $h\nu$ is the photon energy, $P_{\rm opt}$ is the absorbed optical power, and A and B are the fitting parameters. On the other hand, the photoconductive effect shows the linear dependence, which can be written as [15]

$$I_{\rm PC} = q\left(\frac{\eta P_{\rm opt}}{h\nu}\right) \cdot G_{\rm pc} = G_{\rm pc} \cdot I_{\rm primary} = C \cdot P_{\rm opt} \tag{2}$$

where $I_{\rm PC}$ is the photocurrent by the photoconductive effect, $G_{\rm pc}$ is the photoconductor gain, $I_{\rm primary}$ is the primary photocurrent, and C is the fitting parameter.

As shown in Fig. 4, photocurrents for both turn-on (-•-) and turn-off (-○-) states as a function of incident optical powers are measured and fitted to (1) and (2), respectively. The points are measured data and the solid lines are fitted results. The well-fitted lines confirm the identification that the photovoltaic effect is dominant at the turn-on state and the photoconductive effect is dominant at the turn-off state.

Fig. 5 shows the optical modulation responses of the InP HEMT under turn-on and turn-off states at fixed $V_{\rm DS}$ of 0.5 V. Measurements were performed by using a 40-Gb/s external optical modulator and a network analyzer (HP8720D) after careful calibration of characterization setup. Under turn-on state ($V_{\rm GS} = -0.9$ V), the InP HEMT shows a large photoresponse due to the internal gain provided by the photovoltaic effect. However, the photoresponse has relatively small optical 3-dB bandwidth of approximately 580 MHz because the photovoltaic effect is dominated by a long lifetime of photogenerated holes accumulated beneath the source area. On the other hand, the optical modulation response at turn-off state ($V_{\rm GS} = -2$ V) is small, but does not fall off as fast because the photoconductive effect is dominated by photogenerated electrons having a much short lifetime. In this condition, the InP HEMT operates as a photoconductor having an InGaAs optical absorption layer [16].

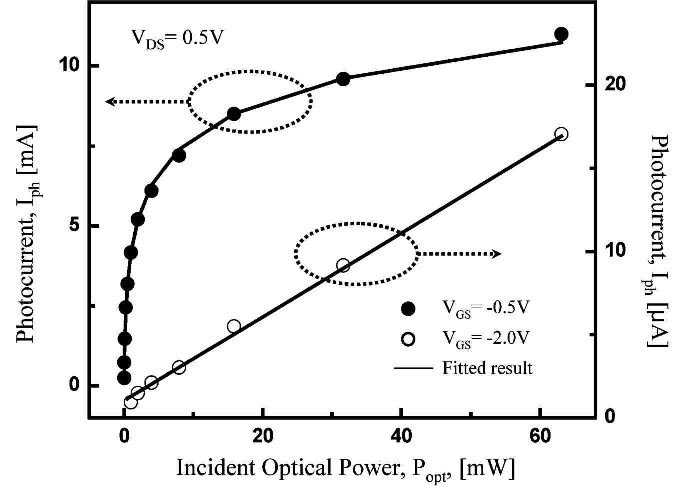

Fig. 4. Photocurrent as a function of incident optical power to the HEMT under turn-on ($V_{\rm GS} = -0.5$ V) and turn-off ($V_{\rm GS} = -2$ V) states. The symbols are measured data and solid lines are fitted results according to (1) and (2).

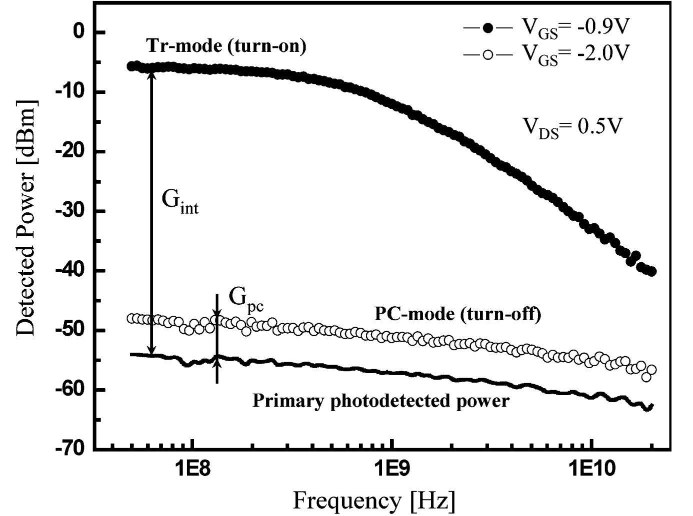

Fig. 5. Measured optical modulation response of the InP HEMT under $V_{\rm GS}$ of -0.9 V (turn-on) and -2 V (turn-off) at fixed $V_{\rm DS}$ of 0.5 V. The solid line is the primary photodetected power extracted from measured data at the turn-off state. $G_{\rm int}$ and $G_{\rm pc}$ represent the phototransistor internal gain and photoconductor gain, respectively.

Phototransistor internal gain is defined as the ratio of amplified photocurrent $(I_{\rm PV})$ to the primary photocurrent $(I_{\rm primary})$ without any internal gain. As described in (2), primary photocurrent can be determined by measuring photocurrent $(I_{\rm PC})$ at the turn-off state and calculating the photoconductor gain $(G_{\rm pc})$. The photoconductor gain can be expressed as [14]

$$G_{\rm pc} = \frac{I_{\rm PC}}{I_{\rm primary}} = \frac{\tau_n}{t_n} = \frac{t_p}{t_n} \approx \frac{v_n}{v_p} \tag{3}$$

where $I_{\rm primary}$ is the primary photocurrent, which indicates actually absorbed optical power in the HEMT, τ_n is the electron lifetime, t_n is the electron transit time, t_p is the hole transit time, v_n is the electron velocity, and v_p is the hole velocity in the channel. In (3), the electron lifetime can be replaced with the

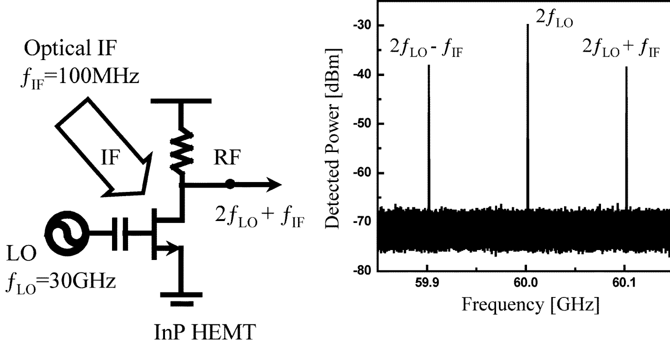

Fig. 6. Utilization of InP HEMT-based phototransistor as a harmonic optoelectronic mixer and its 60-GHz frequency up-conversion spectrum under application of a 30-GHz LO and 100-MHz optical IF signals.

hole transit time because electrons are not supplied from the source until holes arrive at the source region [12]. The ratio of electron and hole transit times can be determined by the ratio of electron to hole velocities in the strained $In_{0.65}Ga_{0.35}As$ channel under an identical electric field [17]. We estimate the photoconductor current gain of approximately two from [17] and [18]. From these results, the primary photodetected powers are determined as shown in Fig. 5. The difference between them and photodetected powers at the turn-on state indicates the phototransistor internal gain (G_{int}). In our experiments, 45-dB phototransistor internal gain is obtained at 100-MHz optical modulation frequency. For its practical applications, including optoelectronic mixers and optically injection-locked oscillators, the InP HEMT should be operated at the turn-on state for providing internal gain. These optical modulation responses directly affect the photodetection bandwidth of optically transmitted IF with data. It can be seen that IF up to the gigahertz range have high internal gain, which should be sufficient for many applications.

III. Harmonic Optoelectronic Up-Conversion to 60-GHz Band

Incorporating these photodetection characteristics with device intrinsic nonlinearities, HEMT-based phototransistors can be utilized as optoelectronic mixers by applying an LO to the gate port [8], [19]. The LO frequency multiplication function can be added, which allows less stringent use of high-frequency LOs, resulting in a harmonic optoelectronic mixer [20]. Fig. 6 shows the schematic diagram for utilizing the InP HEMT as a harmonic optoelectronic mixer and its up-converted output spectrum at 60 GHz. It can be seen that there are harmonic optoelectronic mixing products at $2f_{\mathrm{LO}} + f_{\mathrm{IF}}$ (60.1 GHz) and $2f_{\mathrm{LO}} - f_{\mathrm{IF}}$ (59.9 GHz) and a second harmonic of the LO at $2f_{\mathrm{LO}}$ (60 GHz) under application of a 30-GHz LO to the gate port and 100-MHz optical IF signal. With this harmonic optoelectronic up-conversion scheme, a lower frequency LO can be used making the implementation of a base station easier.

Operation principle of an InP HEMT optoelectronic mixer is identified as follows. As described in Section II, the dominant photodetection mechanism to contribute to phototransistor internal gain in the InP HEMT is the photovoltaic effect which appears in the threshold voltage shift of $I_D - V_{\mathrm{GS}}$ curves. When low-power optical signals are illuminated to the HEMT, the photovoltage (V_{ph}), which is linearly proportional to the absorbed optical power (P_{opt}), is given as

$$V_{\mathrm{ph}} \approx a_1 P_{\mathrm{opt}}. \tag{4}$$

When the LO signal is applied to gate port, frequency mixing between the LO and optical signal occurs by device intrinsic nonlinearity. Although an HEMT has many nonlinear parameters in its equivalent-circuit model, the predominant one for optoelectronic mixing is considered to be nonlinear characteristics of the $I_D - V_{\mathrm{GS}}$ relationship because the input optical signal can be regarded as another voltage input signal to the gate port [8], [20].

The I_D of an HEMT can be written as

$$I_D = I_S + b_1 V_{\mathrm{GS}} + b_2 V_{\mathrm{GS}}^2 + b_3 V_{\mathrm{GS}}^3 + \cdots \tag{5}$$

where $b_{1,\ldots,n}$ are the Taylor series coefficients and I_S is the static drain current. The optical power of the IF modulated lightwave is described by

$$P_{\mathrm{opt}} = P_0 \left[1 + m \cos(2\pi f_{\mathrm{IF}} t)\right] \tag{6}$$

where P_0 is the average optical power and m is the optical modulation index. Considering the LO signal applied to the gate port and optical signal, which is converted to photovoltage (V_{ph}), V_{GS} in (5) can be modified as

$$V_{\mathrm{GS}} = V_{\mathrm{GB}} + V_S \cos(2\pi f_{\mathrm{LO}} t) + V_{\mathrm{ph}} \cos(2\pi f_{\mathrm{IF}} t) \tag{7}$$

where V_{GB} is the dc gate bias voltage and V_S and f_{LO} are the amplitude and frequency of the LO, respectively. By substituting (6) and (7) into (5), the optoelectronic mixing products at $f_{\mathrm{LO}} + f_{\mathrm{IF}}$ and $2f_{\mathrm{LO}} + f_{\mathrm{IF}}$ can be obtained as

$$I_D(f_{\mathrm{LO}} + f_{\mathrm{IF}}) \propto a_1 m P_0 \cdot b_2 V_S \tag{8}$$

$$I_D(2f_{\mathrm{LO}} + f_{\mathrm{IF}}) \propto a_1 m P_0 \cdot b_3 V_S. \tag{9}$$

Since b_2 and b_3 are strongly dependent on dc gate bias voltage V_{GB}, the mixing efficiencies of the desired frequency components can be controlled by changing the gate bias condition.

In order to obtain maximum performance of InP HEMT harmonic optoelectronic mixers, dc-bias conditions are optimized considering conversion efficiency. In the case of a microwave mixer, the conversion gain, which is the ratio of the input IF signal power to the output RF power, is used as an important parameter representing mixer performance. Unfortunately, the same definition cannot be used in an optoelectronic mixer based on an HEMT since the actually absorbed optical IF power is not accurately known. Instead, we define the internal conversion gain as the power ratio of optoelectronic mixing signal to the primary photodetected signal without internal gain, which can be estimated from the measured data at the turn-off state, as mentioned previously. Fig. 7 shows the optoelectronic mixing products at $f_{\mathrm{LO}} + f_{\mathrm{IF}}$ and $2f_{\mathrm{LO}} + f_{\mathrm{IF}}$ and their internal conversion gain as a function of V_{GS}. For its characterization, a 30-GHz LO with 0-dBm power was connected to the gate port and the output signals from the drain port were measured by an RF spectrum analyzer incorporated with an external A-band (Agilent 11970

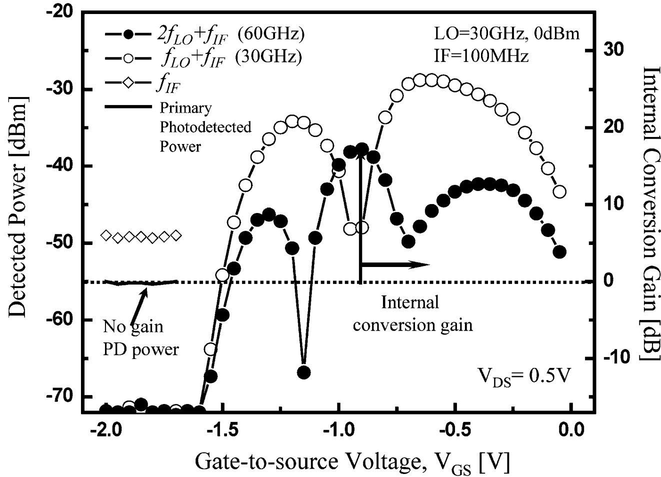

Fig. 7. Dependence of optoelectronic up-converted signals at $f_{\rm LO} + f_{\rm IF}$ and $2f_{\rm LO} + f_{\rm IF}$ on $V_{\rm GS}$ under application of a 30-GHz 0-dBm LO to the gate port and 100-MHz optical IF signals at $V_{\rm DS}$ of 0.5 V. The solid line indicates the primary photodetected power extracted from measured data at the turn-off state. The internal conversion gain defined as the ratio of output up-converted signal powers to the primary photodetected power is also included.

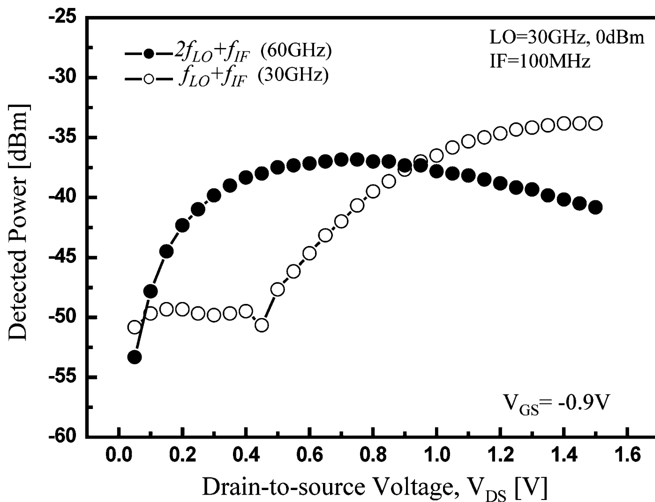

Fig. 8. Dependence of optoelectronic up-converted signals at $f_{\rm LO} + f_{\rm IF}$ and $2f_{\rm LO} + f_{\rm IF}$ on $V_{\rm DS}$ under application of a 30-GHz 0-dBm LO and 100-MHz optical IF signals at $V_{\rm GS} = -0.9$ V.

A) and V-band (Agilent 11 974 V) harmonic mixers. An optical 100-MHz IF signal was illuminated. The primary photodetected $f_{\rm IF}$ signal power of -55 dBm was extracted from the photodetected power measured at $V_{\rm GS}$ of -2 V. It should be noted that the mixing products at $2f_{\rm LO}+f_{\rm IF}$ can be selectively enhanced at $V_{\rm GS}$ of -0.9 V while suppressing undesired mixing components at $f_{\rm LO} + f_{\rm IF}$. This feature is advantageous for an InP HEMT harmonic optoelectronic mixer where the $2f_{\rm LO} + f_{\rm IF}$ product is utilized. In our experiment, 17-dB internal conversion gain is obtained for 60-GHz harmonic optoelectronic up-conversion by setting the optimum $V_{\rm GS}$ of -0.9 V.

For further investigation of the bias condition, we measure the dependence of mixing products at $2f_{\rm LO} + f_{\rm IF}$ and $f_{\rm LO} + f_{\rm IF}$ on $V_{\rm DS}$, as shown in Fig. 8. In the linear mode where $V_{\rm DS}$ is low, the harmonic optoelectronic mixing products at $2f_{\rm LO} + f_{\rm IF}$ are enhanced. However, in the saturation mode, it begins to decrease as increasing $V_{\rm DS}$. The experimental results correspond to the

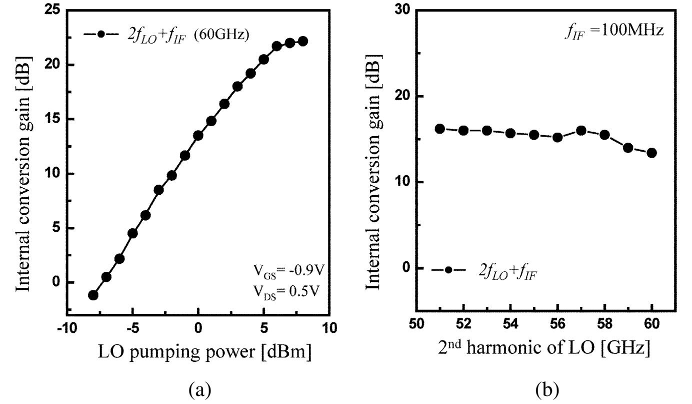

Fig. 9. Dependences of: (a) LO pumping power and (b) applied LO frequency on the internal conversion gain.

characteristics of microwave mixer in which harmonics of LO become strong under the linear mode of the FET [21].

LO pumping power determines the conversion efficiency in a frequency mixer. Fig. 9(a) indicates the internal conversion gain of the harmonic optoelectronic mixing product at $2f_{\rm LO} + f_{\rm IF}$ as a function of LO pumping power under optimum bias conditions. The required LO power to achieve positive internal conversion gain is approximately -7 dBm. When the LO power is higher than 6 dBm, it is observed that internal conversion gain begins to saturate. The LO frequency range of the harmonic optoelectronic mixer is also investigated for its uses at V-band. However, measurement was only taken from 50 to 60 GHz since millimeter-wave components in the experimental setup were not guaranteed above 60 GHz. As observed in Fig. 9(b), the InP HEMT harmonic optoelectronic mixer exhibits wide LO frequency ranges while maintaining high internal conversion gain, which are expected to be sufficient for millimeter-wave operation.

IV. 60-GHz Radio-on-Fiber System Demonstration

In order to investigate the feasibility of using an InP HEMT harmonic optoelectronic mixer in a radio-on-fiber system, broad-band data transmission is demonstrated in both fiber-optic and 60-GHz wireless links. Fig. 10 describes the constructed remote up-conversion 60-GHz radio-on-fiber system using an InP HEMT harmonic optoelectronic mixer. The DFB laser diode having the wavelength of 1552 nm was directly modulated with 622-Mb/s nonreturn-to-zero (NRZ) pseudorandom bit sequence having the pattern length of $2^{15}-1$. The baseband optical data signal was transmitted from the central station to base station over a 30-km single-mode fiber, and frequency up-converted to 60-GHz band using an InP HEMT harmonic optoelectronic mixer with the optimum bias conditions and a 30-GHz 1-dBm LO. The output signal at the drain port was amplified by a 17-dB post-amplifier and radiated from a 60-GHz horn antenna with 20-dB gain. Fig. 11 shows the 60-GHz spectrum of frequency up-converted 622-Mb/s data measured at the output of the amplifier. After 3-m wireless transmission, the received signals were demodulated using a direct detection technique with a Schottky diode. The recovered baseband signals were filtered and connected to a sampling

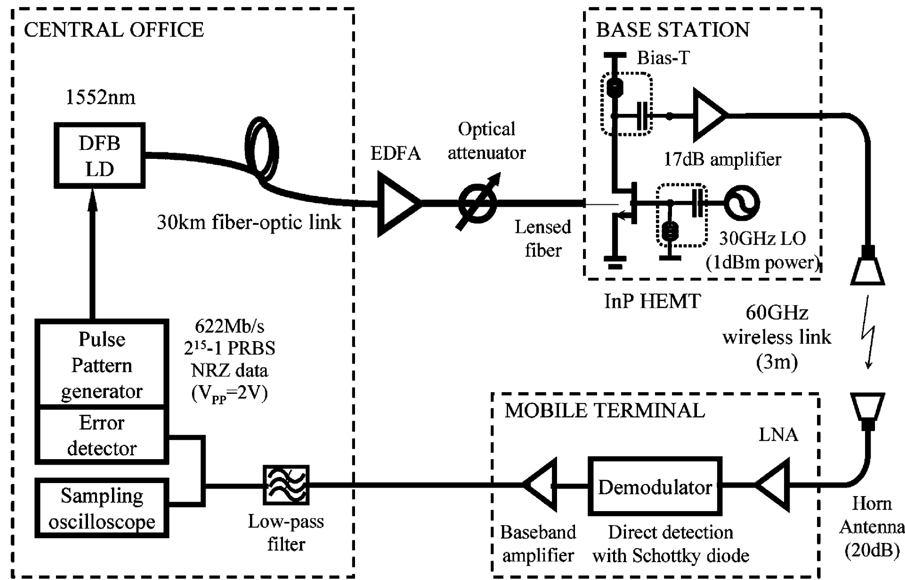

Fig. 10. 60-GHz remote up-conversion radio-on-fiber system utilizing an InP HEMT as a harmonic optoelectronic mixer.

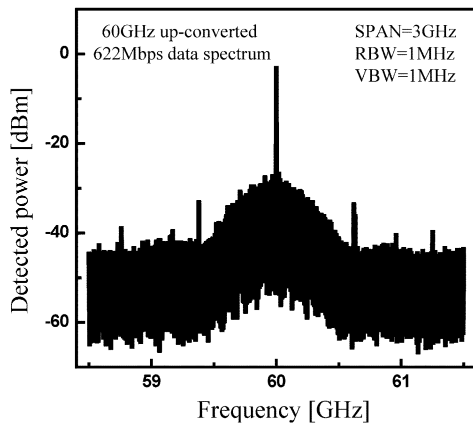

Fig. 11. Measured 60-GHz spectrum of frequency up-converted 622-Mb/s signal.

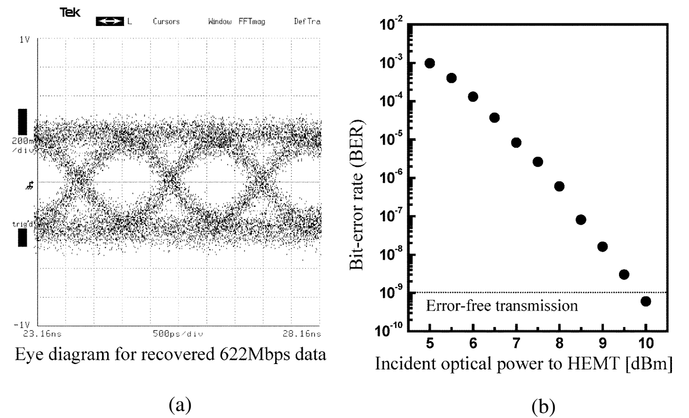

Fig. 12. (a) Eye diagram for recovered 622-Mb/s data after transmission over 30-km single-mode fiber and 3-m free-space at 60-GHz band. (b) BER characteristics as a function of incident optical power to an HEMT. The absorbed optical power is estimated to be less than 10% of the incident optical power.

oscilloscope for eye diagram measurement or error detector for bit error rate (BER) measurement.

Clear eye opening for recovered 622-Mb/s data is observed as shown in Fig. 12(a). The link performance was evaluated by measuring the BER as a function of incident optical power. Fig. 12(b) shows the experimental results for BER characteristics of a constructed radio-on-fiber system. Error-free transmission (BER $< 10^{-9}$) was achieved at 9-dBm incident optical power to the InP HEMT. Comparing the BER characteristics of 30-km fiber-optic links with those of back-to-back links, there is no significant transmission penalty at identical incident optical power. The results affirms the fact that remote up-conversion systems are free from the chromatic dispersion induced transmission penalty because low-frequency optical IF or baseband data propagates through optical fiber [4]. Since the actually absorbed optical power is less than 10% of incident optical power, as mentioned before, the required optical power for error-free transmission can be significantly decreased if more efficient optical coupling techniques are utilized.

V. Conclusion

We have investigated the phototransistor based on an InP HEMT and have demonstrated a millimeter-wave radio-on-fiber system by utilizing it as a harmonic optoelectronic mixer. The physical origins for photodetection in an InP HEMT are classified into two major effects, i.e., photovoltaic effect and photoconductive effect. The former provides an InP HEMT with internal gain at the turn-on state; on the other hand, the latter observed at turn-off state makes it possible to estimate the primary photocurrent that corresponds to the actually absorbed optical power. Phototransistor internal gain was determined by

taking the difference between them and including photoconductor gain. In addition, it was demonstrated that InP HEMT-based phototransistors can be used as harmonic optoelectronic mixers, which were experimentally characterized at the 60-GHz band. The performance was evaluated in terms of internal conversion gain, which directly indicates conversion efficiency in an optoelectronic mixer. In order to demonstrate their feasibility, 622-Mb/s data transmission was achieved in a radio-on-fiber system, which consists of 30-km fiber-optic link and 3-m wireless link at 60 GHz. Since the InP HEMT gives many functionalities and the possibility of integration with the other RF components, it is expected to contribute to the realization of simple base stations in radio-on-fiber systems.

REFERENCES

[1] A. J. Seeds, "Microwave photonics," *IEEE Trans. Microw. Theory Tech.*, vol. 50, no. 3, pp. 877–887, Mar. 2002.

[2] L. Noel, D. Wake, D. G. Moodie, D. D. Marcenac, L. D. Westbrook, and D. Nesset, "Novel techniques for high-capacity 60 GHz fiber-radio transmission systems," *IEEE Trans. Microw. Theory Tech.*, vol. 45, no. 8, pp. 1416–1423, Aug. 1997.

[3] T. Kuri, K.-I. Kitayama, A. Stohr, and Y. Ogawa, "Fiber-optic millimeter-wave downlink system using 60 GHz-band external modulation," *J. Lightw. Technol.*, vol. 17, no. 5, pp. 799–806, May 1999.

[4] U. Gliese, S. Norskov, and T. N. Nielsen, "Chromatic dispersion in fiber-optic microwave and millimeter-wave links," *IEEE Trans. Microw. Theory Tech.*, vol. 41, no. 10, pp. 1716–1724, Oct. 1996.

[5] H. Kamitsuna, Y. Matsuoka, S. Yamahata, and N. Shigekawa, "Ultra-high-speed InP/InGaAs DHPT for OEMMIC," *IEEE Trans. Microw. Theory Tech.*, vol. 49, no. 10, pp. 1921–1925, Oct. 2001.

[6] J. Lasri, A. Bilenca, G. Eisenstein, and D. Ritter, "Optoelectronic mixing, modulation and injection-locking in millimeter-wave self-oscillating InP/InGaAs heterojunction bipolar phototransistors—Single and dual transistor configuration," *IEEE Trans. Microw. Theory Tech.*, vol. 49, no. 10, pp. 1934–1939, Oct. 2001.

[7] E. Suematsu and N. Imai, "A fiber-optic/millimeter-wave radio transmission link using HBT as direct photodetector and an optoelectronic up-converter," *IEEE Trans. Microw. Theory Tech.*, vol. 44, no. 1, pp. 133–143, Jan. 1996.

[8] A. Paolella, S. Malone, T. Berceli, and P. R. Herczfeld, "MMIC compatible lightwave-microwave mixing techniques," *IEEE Trans. Microw. Theory Tech.*, vol. 43, no. 3, pp. 518–522, Mar. 1995.

[9] C. Rauscher and K. J. Williams, "Heterodyne reception of millimeter-wave modulated optical signals with an InP-based transistor," *IEEE Trans. Microw. Theory Tech.*, vol. 42, no. 11, pp. 2027–2034, Nov. 1994.

[10] J. C. Campbell, "Phototransistors for lightwave communication," in *Semiconductors and Semimetals, Lightwave Communications Technology*. Orlando, FL: Academic, 1985, pt. D, vol. 22, pp. 389–447.

[11] Y. Yamashita, A. Endoh, K. Shinohara, K. Hikosaka, T. Matsui, S. Hiyamizu, and T. Mimura, "Pseudomorphic $In_{0.52}Al_{0.48}As/In_{0.7}Ga_{0.3}As$ HEMT's with an ultrahigh f_T of 562 GHz," *IEEE Electron Device Lett.*, vol. 23, no. 10, pp. 573–575, Oct. 2002.

[12] Y. Takanashi, K. Takahata, and Y. Muramoto, "Characteristics of InAlAs/InGaAs high-electron-mobility transistors under illumination with modulated light," *IEEE Trans. Electron Devices*, vol. 46, no. 12, pp. 2271–2277, Dec. 1999.

[13] C.-S. Choi, H.-S. Kang, W.-Y. Choi, H.-J. Kim, W.-J. Choi, D.-H. Kim, K.-C. Jang, and K.-S. Seo, "High optical responsivity of InAlAs-InGaAs metamorphic high-electron mobility transistor on GaAs substrate with composite channel," *IEEE Photon. Technol. Lett.*, vol. 15, no. 6, pp. 846–848, Jun. 2003.

[14] H.-S. Kang, C.-S. Choi, W.-Y. Choi, D.-H. Kim, and K.-S. Seo, "Characterization of phototransistor internal gain in metamorphic high-electron-mobility transistors," *Appl. Phys. Lett.*, vol. 84, no. 19, pp. 3780–3782, May 2004.

[15] S.-L. Chuang, *Physics of Optoelectronic Devices*. New York: Wiley, 1995.

[16] J. C. Gammel, H. Ohno, and J. M. Ballantyne, "High-speed photoconductive detectors using GaInAs," *IEEE J. Quantum Electron.*, vol. 17, no. 2, pp. 269–272, Feb. 1981.

[17] K. Brennan, "Theory of the steady-state hole drift velocity in InGaAs," *Appl. Phys. Lett.*, vol. 51, no. 13, pp. 995–997, Sep. 1987.

[18] J. L. Thobel, L. Baudry, A. Cappy, P. Bourei, and R. Fauquembergue, "Electron transport properties of strained $In_xGa_{1-x}As$," *Appl. Phys. Lett.*, vol. 56, no. 4, pp. 346–348, Jan. 1990.

[19] H. Kamitsuna and H. Ogawa, "Monolithic image-rejection optoelectronic up-converter that employ the MMIC process," *IEEE Trans. Microw. Theory Tech.*, vol. 41, no. 12, pp. 2323–2329, Dec. 1993.

[20] C.-S. Choi, H.-S. Kang, W.-Y. Choi, D.-H. Kim, and K.-S. Seo, "Characteristics of InP HEMT harmonic optoelectronic mixers and their applications to 60 GHz radio-on-fiber system," in *IEEE MTT-S Int. Microwave Symp. Dig.*, Fort Worth, TX, Jun. 2004, pp. 401–404.

[21] S. A. Mass, *Microwave Mixers*. Boston, MA: Artech House, 1993.

Chang-Soon Choi (S'01) was born in Seoul, Korea, on February 25, 1977. He received the B.S. and M.S. degrees in electrical and electronic engineering from Yonsei University, Seoul, Korea, in 1999 and 2001, respectively, and is currently working toward the Ph.D. degree at Yonsei University. His doctoral dissertation concerns high-speed InP phototransistors and their applications to radio-on-fiber technologies.

His other research interests include optical generation of millimeter-wave, terahertz optoelectronics, and silicon-based optoelectronic integrated circuits.

Hyo-Soon Kang was born in Seoul, Korea, in 1978. He received the B.S. and M.S. degrees in electrical and electronic engineering from Yonsei University, Seoul, Korea, in 2002 and 2004, respectively, and is currently working toward the Ph.D. degree at Yonsei University. His master's thesis concerns the investigation of photodetection characteristics of HEMTs and their applications for radio-on-fiber systems.

His research interests include microwave photonics and optical receivers based on the CMOS process.

Woo-Young Choi (S'98–M'92) received the B.S., M.S., and Ph.D. degrees in electrical engineering and computer science from the Massachusetts Institute of Technology (MIT), Cambridge, in 1986, 1988, and 1994, respectively. His doctoral dissertation concerned MBE-grown InGaAlAs laser diodes for fiber-optic applications.

From 1994 to 1995, he was a Post-Doctoral Research Fellow with National Telephone and Telegraph (NTT) Opto-Electronics Laboratories, where he was involved with femtosecond all-optical switching devices. In 1995, he joined the Department of Electrical and Electronic Engineering, Yonsei University, Seoul, Korea, where he is currently an Associate Professor. His research interest is in the area of high-speed information processing technology, which includes high-speed optoelectronics, high-speed electronic circuits, and microwave photonics.

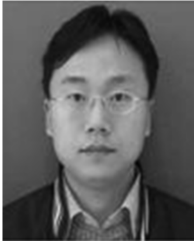

Dae-Hyun Kim was born in Taegu, Korea, on November 13, 1974. He received the B.S. degree in electrical engineering and computer science from Kyung-Pook National University, Taegu, Korea, in 1997, the M.S. degree from electrical engineering and Ph.D. degree on electrical engineering and computer science from Seoul National University, Seoul, Korea, in 2000 and 2004, respectively.

He is current a Post-Doctorate with the Department of Electrical Engineering and Computer Science, Seoul National University From 1999 to 2001, he was a Research Assistant with the Inter-University Semiconductor Research Center (ISRC), Seoul, Korea, where he was engaged in the development of 0.5-mm CMOS fabrication for dry etching. His current interests include the development for the III–V nano-InGaAs-HEMT device and its application for high-speed digital and analog integrated circuits.

Kwang-Seok Seo received the B.S. degree from Seoul National University, Seoul, Korea, in 1976, the M.S. degree from the Korea Advanced Institute of Science and Technology, Daejun, Korea, in 1978, and the Ph.D. degree in electrical engineering from The University of Michigan at Ann Arbor, in 1987.

From 1978 to 1982, he was Senior Research Engineer with the Korea Institute of Electronics Technology. From 1987 to 1988, he was a Post-Doctoral Fellow with the IBM T. J. Watson Research Center. Since 1989, he has been with the Seoul National University, where he is currently a Professor with the School of Electrical Engineering and Computer Science. His current interests include high-speed device physics and technology, compound semiconductor materials, and high-frequency circuit design.